Active and stable platinum/ionic liquid/carbon nanotube electrocatalysts for oxidation of methanol

Guan-Lin Lin, Arun Prakash Periasamy, Zih-Yu Shih, and Huan-Tsung Chang*

Department of Chemistry, National Taiwan University, 1, Section 4, Roosevelt Road, Taipei 106, Taiwan
*Corresponding author's e-mail address: changht@ntu.edu.tw

Published online: October 9, 2014 (version 1)
Cite as: Lin et al., ScienceOpen Research 2014 (DOI: 10.14293/S2199-1006.1.SORCHEM.AYZQJS.v1)
Reviewing status: Please note that this article is under continuous review. For the current reviewing status and the latest referee's comments please click **here** or scan the QR code at the end of this article.

Primary discipline: Chemistry
Keywords: Imidazolium ionic liquids, Platinum nanoparticles, Carbon nanotubes, Methanol oxidation reaction, Anode catalyst

ABSTRACT

Platinum (Pt) nanoparticles (NPs) on carbon nanotubes (CNTs) from $PtCl_6^{2-}$ ions through a facile ionic liquid (IL)-assisted method has been developed and used for methanol oxidation. 1-Butyl-3-methylimidazolium (BMIM) with four different counter ions (PF_6^-, Cl^-, Br^-, and I^-) have been tested for the preparation of Pt/IL/CNT nanohybrids, showing the counterions of ILs play an important role in the formation of small sizes of Pt NPs. Only [BMIM][PF_6] and [BMIM][Cl] allow reproducible preparation of Pt/IL/CNT nanohybrids. The electroactive surface areas of Pt/[BMIM][PF_6]/CNT, Pt/[BMIM][Cl]/CNT, Pt/CNT, and commercial Pt/C electrodes are 62.8, 101.5, 78.3, and 87.4 m^2 g^{-1}, respectively. The Pt/[BMIM][Cl]/CNT nanohybrid-modified electrodes provide higher catalytic activity (251.0 A g^{-1}) at a negative onset potential of -0.60 V than commercial Pt/C-modified ones do (133.5 A g^{-1}) at -0.46 V. The Pt/[BMIM][Cl]/CNT electrode provides the highest ratio (4.52) of forward/reverse oxidation current peak, revealing a little accumulation of carbonaceous residues.

INTRODUCTION

Various morphologies of platinum (Pt) nanomaterials (NMs) with large surface areas and high surface energies have been widely used as catalysts for enhanced methanol oxidation reaction (MOR) in direct methanol fuel cells (DMFCs) [1, 2]. In order to further enhance efficiency of DMFCs through accelerating the electron transfer rate, carbon nanotubes (CNTs) with properties of high specific surface areas, electrical conductivities, and chemical stability have been used as supports for the preparation of Pt nanoparticles (NPs)/CNT nanohybrids [3–7]. However, pristine CNTs have insufficient binding sites to anchor Pt ions (precursors) and NPs, which usually leads to poor dispersion and the formation of NPs aggregates [8]. As a result, inefficient catalytic activity, irreproducibility, and poor durability of Pt NPs/CNT nanohybrids occur.

In order to produce more efficient and reliable Pt NPs/CNT nanohybrids, functional CNTs with greater binding sites and surface anchoring groups are usually used [9]. Acid oxidation is a common approach to produce CNTs with greater binding sites (CO, COH, and COOH groups) on their surfaces that can anchor great amounts of Pt ions and Pt NPs [10, 11]. However, this method typically results in an uneven distribution of surface functional groups as well as severe structural damage to CNTs. Safety of using strong acid to treat CNTs at elevated temperature is a concern. Alternatively, electrochemical oxidation of CNTs at their defect sites is used to produce quinonyl, carboxyl, or hydroxyl groups on their surfaces [12–14]. Chemical modification of CNTs with molecules such as water-soluble polymers, quaternary ammonium salts, surfactants, and polyoxoanions has become popular for preparation of functional CNTs, mainly because of easy operation in aqueous solution and purification [15]. However, changes in the aromatic structures of CNTs sometimes occurs [16]. With various degrees of π-conjugates (C=C) on their surfaces, CNTs conjugated with aromatic compounds such as pyrene through π-π stacking is also common. Although modification of CNTs can be achieved without altering their structure under mild reaction conditions [17], weak π-π stacking force between molecules and CNTs might cause reproducibility and durability problems.

Having excellent properties of good chemical and thermal stability, almost negligible vapor pressure, good electrical conductivity, and a wide electrochemical window [18, 19], ionic liquids (ILs) have been found useful for the modification of CNTs [1, 20]. In addition, ILs are also useful solvents and stabilizers for the preparation of various metal NPs, mainly because of having high intrinsic charges that allow them to stabilize metal NPs through electrostatic attractions [21–23]. Having such excellent properties to stabilize CNTs and Pt NPs [24], it is worthy to test the possibility of preparing Pt NPs/CNT nanohybrids in the presence of ILs.

To prepare Pt NPs/CNT nanohybrids, 1-butyl-3-methylimidazolium (BMIM)-based ILs with various counterions were tested, including [BMIM][PF_6], [BMIM][Cl], [BMIM][Br], and [BMIM][I]. The BMIM-based ILs were adsorbed onto the surfaces of CNTs to provide great amount of surface functional groups on their surfaces to stabilize Pt^{4+} ions that were then reduced to form well-distributed Pt NPs by ethylene glycol. The IL film on the CNTs also provided great amounts of positive charges that prevented aggregation of the as-prepared Pt NPs/CNT nanohybrids. The as-prepared Pt/[BMIM][Cl]/CNT nanohybrids possessed enhanced electrocatalytic activity and stability toward MOR when compared with the nanohybrids prepared without ILs, showing their great potential in DMFCs.

EXPERIMENTAL

Materials

CNTs (10–30 nm in diameter) were purchased from Seedchem Company Pty. Ltd. (Melbourne, Australia). [BMIM][PF_6] (≥98.0 wt%) and [BMIM][Cl] (≥98.0 wt%) were obtained separately from Acros Organics (Geel, Belgium) and Tokyo Chemical Industry (Tokyo, Japan). N, N-dimethylformamide (DMF, ≥99.8 wt%) was purchased from Sigma-Aldrich (Milwaukee, WI). Ethylene glycol (≥99.9 wt%) was purchased from J. T. Baker (Phillipsburg, NJ, USA). [BMIM][Br] (≥99.0 wt %) and Pt on activated carbon (40 wt% Pt) were obtained from Alfa Aesar (Ward Hill, MA, USA). [BMIM][I] (≥98.0 wt%) was purchased from UniRegion Bio-Tech (Taipei, Taiwan). Potassium hexachloroplatinate (IV) was obtained from J & J Materials (Neptune City, New Jersey). Methanol (≥99.8 wt%) was purchased from Sigma (St. Louis, MO, USA). Nafion 117 (5 wt%) was purchased from Fluka (Buchs, Switzerland). Screen-printed electrodes (No. SE101-GK) were obtained from Zensor R & D (Taichung, Taiwan). Highly purified water (18.2 MΩ-cm) from a Milli-Q ultrapure system (London, UK) was used throughout this study.

Preparation of Pt/ILs/CNT nanohybrids

Four ILs, including [BMIM][PF_6], [BMIM][Cl], [BMIM][Br], and [BMIM][I], were used separately to prepare Pt/ILs/CNT nanohybrids. A representative reaction procedure is described. CNT (0.4 mg) and [BMIM][PF_6] (400 μL, 4%) were mixed with DMF, with a final volume of 10.0 mL. The solution was subjected to sonication for 5 min and then excess DMF was removed through centrifugation at a relative centrifugal force (RCF) of 7370 g for 10 min. The black precipitates were added to a mixture of ethylene glycol (5.7 mL) and ultrapure water (2.3 mL). The mixture was subjected to sonication for 5 min and then K_2PtCl_6 (2.0 mL and 0.6 mM) was added to. The reaction mixture was kept at 115°C for 1 h to form Pt/ILs/CNT nanohybrids. The as-prepared Pt/ILs/CNT nanohybrids were finally purified through sonication for 5 min and four cycles of centrifugation (RCF 7370 g, 10 min)/wash (ultrapure water, 4 × 10 mL).

Characterization

Transmission electron microscopy (TEM) and high-resolution TEM (HRTEM) images of as-prepared Pt/ILs/CNT nanohybrids were recorded using JEOL JSM-1230 (Hitachi, Tokyo, Japan) and FEI Tecnai-G2-F20 (GCEMarket, NJ, USA) systems operating at 200 kV, respectively. Energy-dispersive X-ray spectrometer (EDS) equipped with a Hitachi S-4800 field emission scanning electron microanalyzer (Hitachi, Tokyo, Japan) was applied to determine the composition of the as-prepared Pt/ILs/CNT nanohybrids. The X-ray diffraction (XRD) patterns of the as-prepared Pt/ILs/CNT nanohybrids were recorded using a PANalytical X'Pert PRO diffractometer (Almelo, Netherlands) with Cu Kα radiation (λ = 0.15418 nm). X-ray photoelectron spectroscopy (XPS) measurement was conducted to determine Pt oxidation state in the as-prepared Pt/ILs/CNT nanohybrids using a VG ESCA210 electron spectroscope from VG Scientific (West Sussex, UK). The binding energy (BE) for carbon was used as an internal reference to eliminate the charging effect. The samples for XPS measurements were prepared by depositing drops of the as-prepared Pt/ILs/CNT nanohybrids onto Si substrates and then the solvents evaporated at ambient temperature (25°C) and pressure. An Elan 6000 inductively coupled plasma mass spectrometer (ICP-MS) from Perkin–Elmer (Wellesley, MA, USA) was employed to determine Pt contents in the as-prepared Pt/ILs/CNT nanohybrids. Prior to ICP-MS measurements, the as-prepared Pt/ILs/CNT nanohybrids were dissolved in 2% HNO_3.

Fabrication of electrodes and electrocatalytic analysis

Aliquots (5 μL) of the as-synthesized Pt/ILs/CNT nanohybrids solutions were dropped separately onto clean screen-printed electrodes (diameter: 3 mm). After the electrodes were air-dried for 1 h at ambient temperature, Nafion solution (0.5%, 1 μL) was placed onto each of the electrodes. Three-electrode electrochemical cells were fabricated using the modified electrode as a working electrode, a Pt wire as an auxiliary electrode, and an Ag/AgCl electrode as a reference electrode. The electrocatalytic activities of the as-synthesized Pt/ILs/CNT nanohybrids were measured using a CHI 760D electrochemical workstation (Austin, TX, USA). Cyclic voltammetry (CV) measurements in 0.5 M KOH with or without containing 0.5 M methanol were conducted over the potential range from -1.0 to 0.2 V at a scan rate of 100 mV s^{-1}. As a control, commercial Pt/C NPs and as-synthesized Pt/CNT nanohybrids prepared without ILs were used to prepare working electrodes under the same conditions. All electrochemical data were recorded over 50 reproducible cycles. The chronoamperometric measurements for durability tests were conducted in

0.5 M KOH containing 0.5 M methanol at a fixed potential of −0.1 V for 20,000 s.

RESULTS AND DISCUSSION

Formation and characterization of Pt/ILs/CNT nanohybrids

Through the π–π interaction of CNTs with BMIM group of the ILs, CNTs were stabilized in the aqueous solutions. $PtCl_6^{2-}$ ions were then adsorbed on the cationic surfaces of the CNTs through electrostatic attraction [25]. The adsorbed $PtCl_6^{2-}$ ions were reduced by ethylene glycol (reducing agent) to form Pt NPs on the surfaces of CNTs. Having a weaker reducing strength than $NaBH_4$, as well as capability for rapid and homogenous in situ generation of reducing species, ethylene glycol allowed better control of the particle growth, leading to the formation of a fairly uniform Pt NPs on the surfaces of CNTs [26, 27]. The formation of Pt NPs was through reactions (1) and (2) [28]:

$$HOCH_2CH_2OH \rightarrow CH_3CHO + H_2O \tag{1}$$

$$2CH_3CHO + (PtCl_6)^{2-} + 6OH^- \rightarrow 2CH_3COO^- + Pt + 6Cl^- + 4H_2O \tag{2}$$

Figure 1A and 1B show the TEM images of Pt/[BMIM][PF_6]/CNT and Pt/[BMIM][Cl]/CNT nanohybrids, respectively, showing Pt NPs on the surfaces of CNTs. A greater amount and better distribution of Pt NPs on the CNT surface were observed when using [BMIM][PF_6]. The ring patterns of selected-area electron diffraction (SAED) are displayed in the insets to Figure 1A and 1B, respectively, revealing the crystalline structures of Pt (111). HRTEM images of Pt/[BMIM][PF_6]/CNT and Pt/[BMIM][Cl]/CNT nanohybrids in Figure 1C and 1D, respectively, clearly show highly dispersed Pt NPs with a small size distribution on the CNT surface. The lattice spacing of d_{111} for the Pt NPs is 0.22 nm [29]. The average diameters of Pt NPs (200 counts) in the Pt/[BMIM][PF_6]/CNT and Pt/[BMIM][Cl]/CNT nanohybrids were 2.8 ± 0.3 and 2.6 ± 0.2 nm, respectively.

Supplementary Figure S1 displays that the Pt/CNT, Pt/[BMIM][PF_6]/CNT, and Pt/[BMIM][Cl]/CNT nanohybrids all provide the diffraction peaks at 39.5° and 45.7° that are assigned to face central cubic Pt planes (111) and (200), respectively, in reference to JCPDS card No. 87-0646 [30]. The peaks at 25.9°, 42.7°, and 54.2° correspond to the (002), (100), and (004) planes, respectively, of graphitized CNTs, in reference to JCPDS card No. 75-1621 [30]. The results reveal that the as-synthesized nanohybrids consist of pure

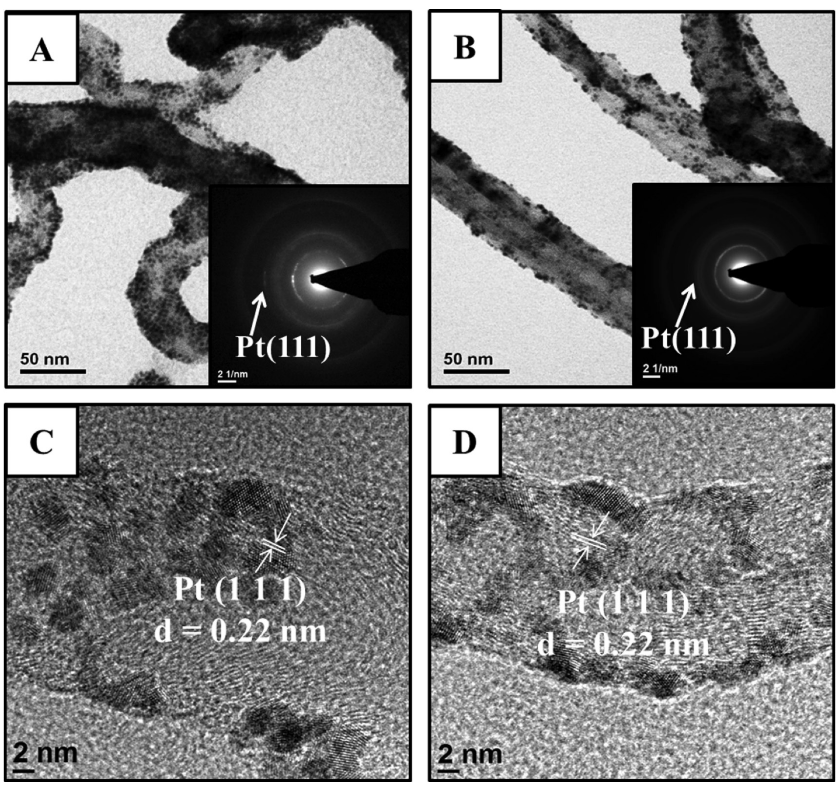

Figure 1. TEM images (A and B) and HRTEM images (C and D) of Pt/[BMIM][PF_6]/CNT and Pt/[BMIM][Cl]/CNT nanohybrids. Inset to (A) and (B): their corresponding SAED patterns.

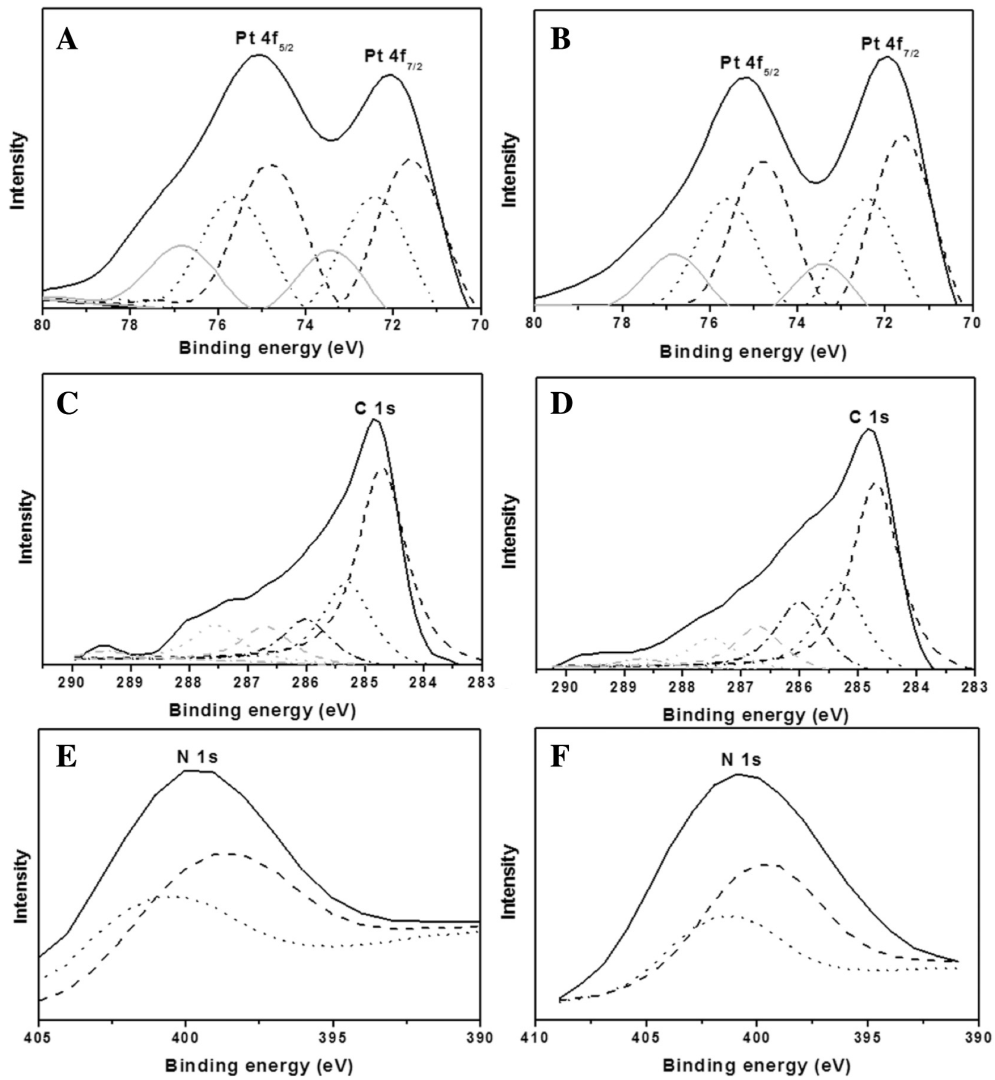

Figure 2. XPS spectra displaying the Pt_{4f} (A and B), C_{1s} (C and D), and N_{1s} (E and F) energy levels of the Pt/[BMIM][PF_6]/CNT (A, C, and E) and Pt/[BMIM][Cl]/CNT (B, D, and F) nanohybrids.

crystalline Pt and CNTs [25]. The XPS spectra depicted in Figure 2A and 2B show a doublet of fitted Pt_{4f} peaks at 71.6 eV ($4f_{7/2}$) and 74.8 eV ($4f_{5/2}$), respectively, which correspond to the metallic Pt [31]. After deconvolution of the peak, six peaks were identified as shown in the dotted curves [26]. The $4f_{7/2}$ peak at 72.4 eV with a $4f_{5/2}$ component at 75.6 eV are attributed to the Pt (II) chemical states of PtO or $Pt(OH)_2$ [31]. The $4f_{7/2}$ peak at 73.4 eV with a $4f_{5/2}$ component at 76.8 eV are attributed to the +4 oxidation state of Pt. Figure 2C and 2D show the curves fitted C_{1s} peak, with a main peak at 284.7 eV that is assigned for the C_{1s} of the sp^2-hybryidized graphitic carbon [32]. A peak at 285.3 eV is assigned to sp^3-hybridized carbon atoms as in diamond-like carbon [32]. We note that these two peaks are observed in amorphous carbons, and their relative intensity correlates with the degree of graphitization [33]. Peaks with higher binding energies located at 286.0, 287.5, and 289.4 eV are assigned to C–O– (e. g., alcohol and ether), >C=O (ketone and aldehyde), –COO– (carboxylic acid and ester) functional groups, respectively [30, 32]. The peak at 286.7 eV is assigned to C–N group from BMIM [34]. We note that the electronegative oxygen atoms induce the formation of more positive charge on a carbon atom. The bonding configurations (Figure 2E and 2F) of the nitrogen atoms in the Pt/[BMIM][PF_6]/CNT and Pt/[BMIM][Cl]/CNT nanohybrids were also fitted. The peak at 399.8 eV in the N_{1s} spectrum corresponds to pyrrole-like nitrogen. When carbon atoms in the CNT surface are substituted by nitrogen atoms in the form of "graphitic" nitrogen, the corresponding peak is located at 401.5 eV [2, 35–37]. The functionalization of CNTs with nitrogen-containing materials is beneficial to enhance the dispersion of Pt NPs on the CNTs due to a strong coordinative interaction between nitrogen atoms and Pt NPs [6, 12, 13].

Electrocatalytic activities of Pt/ILs/CNT nanohybrid-modified electrodes

Before we tested the electroactivity of the as-prepared Pt/ILs/CNT nanohybrids for MOR, we estimated their electroactive surface areas (EASA, $m^2\ g^{-1}$) by conducting CV measurement [38]. The CVs of Pt/ILs/CNT nanohybrid-modified electrodes at a scan rate of 100 mV s^{-1} are displayed in Figure 3A. The EASA of each electrode was calculated using Equation (3):

$$\mathrm{EASA} = Q/(0.21 \times [\mathrm{Pt}]) \tag{3}$$

where [Pt] represents the Pt loading (mg cm^{-2}) in the electrode. EASA were calculated from integrating the charges associated with the hydrogen adsorption–desorption peaks (Q, mC cm^{-2}), assuming 210 μC cm^{-2} needed for a monolayer of H as-atoms in Figure 3A [39]. The EASAs of as-prepared Pt/[BMIM][PF_6]/CNT, Pt/[BMIM][Cl]/CNT and Pt/CNT nanohybrids and commercial Pt/C NPs are 62.8, 101.5, 78.3, and 87.4 $m^2\ g^{-1}$, respectively. The results reveal that the counterions of ILs affected the adsorbed amounts of Pt NPs, mainly because the species of anions, cations, and the length of the lateral alkyl groups on the heterocyclic rings affects the physicochemical properties of ILs [24]. Having a higher steric effect of PF_6^- relative to Cl^-, it is more difficult for $PtCl_6^{2-}$ ions to access the surface of CNTs adsorbed with [BMIM][PF_6], leading to less amounts of the formation of Pt NPs and a smaller EASA value when using [BMIM][PF_6]. Further, the EASA value (101.5 $m^2\ g^{-1}$) of Pt/[BMIM][Cl]/CNT is higher than that of IL (1-octyl-3-methylimidazolium PF_6)-supported $Pt_{0.17}Cu_{0.83}$/graphene (75.6 $m^2\ g^{-1}$), Pt/graphene (49.4 $m^2\ g^{-1}$), $Pt_{0.17}Cu_{0.83}$/carbon black (27.6 $m^2\ g^{-1}$), Pt/carbon black (10.1 $m^2\ g^{-1}$) [40], PtRu/CNTs-PIL (91.2 $m^2\ g^{-1}$), and Pt/CNTs-PIL (71.4 $m^2\ g^{-1}$) [41] catalysts, respectively. Figure 3B shows the CVs of as-prepared Pt/[BMIM][PF_6]/CNT, Pt/[BMIM][Cl]/CNT, Pt/CNT nanohybrids, and commercial Pt/C NPs in a 0.5 M KOH containing 0.5 M methanol at a scan rate of 100 mV s^{-1}. The Pt/[BMIM][Cl]/CNT nanohybrid-modified electrode exhibited a mass activity of 251.0 A g^{-1} for MOR, which is higher than that (126.9 A g^{-1}) of the Pt/[BMIM][PF_6]/CNT nanohybrid-modified electrode. Besides, the mass activity of 251.0 A g^{-1} for the Pt/[BMIM][Cl]/CNT nanohybrid-modified electrode in alkaline solution (0.5 M KOH) is higher than that (242.3 A g^{-1} and 155.7 A g^{-1}) for the PtRu/CNTs-PIL and Pt/CNTs-PIL-modified electrodes [41], respectively, in the acidic solution (0.5 M H_2SO_4), showing that higher EASA and alkaline condition are essential to provide higher mass activity for MOR. It has also been reported that the polarization characteristics of MOR at the unsupported Pt black in alkaline solution is one order higher than that in the acidic solution [42]. The onset potential of MOR on the Pt/[BMIM][Cl]/CNT nanohybrid-modified electrode occurred at near −0.60 V (vs. Ag/AgCl), which is more negative than those of as-prepared Pt/[BMIM][PF_6]/CNT nanohybrids (−0.50 V), Pt/CNT (−0.47 V), commercial Pt/C catalyst (−0.46 V), and Pd/Pt (−0.50 V) [43]. It is likely attributed to the stronger adsorption of chlorine on the Pt (100) surface than that on the Pt(111) surface due to the lower work function of Pt(100) surface [44]. The result reveals that Pt/[BMIM][Cl]/CNT nanohybrid-modified electrode relative to the other tested electrodes provided greater electrooxidation activity toward the MOR [45]. The cathodic oxide reduction peak for the Pt/[BMIM][Cl]/CNT nanohybrids occurred at −0.48 V (Figure 3A), which is at least 0.05 V higher relative to that of the other tested catalysts, showing their less-favorable formation of Pt-OH [46]. A fast charge transfer through

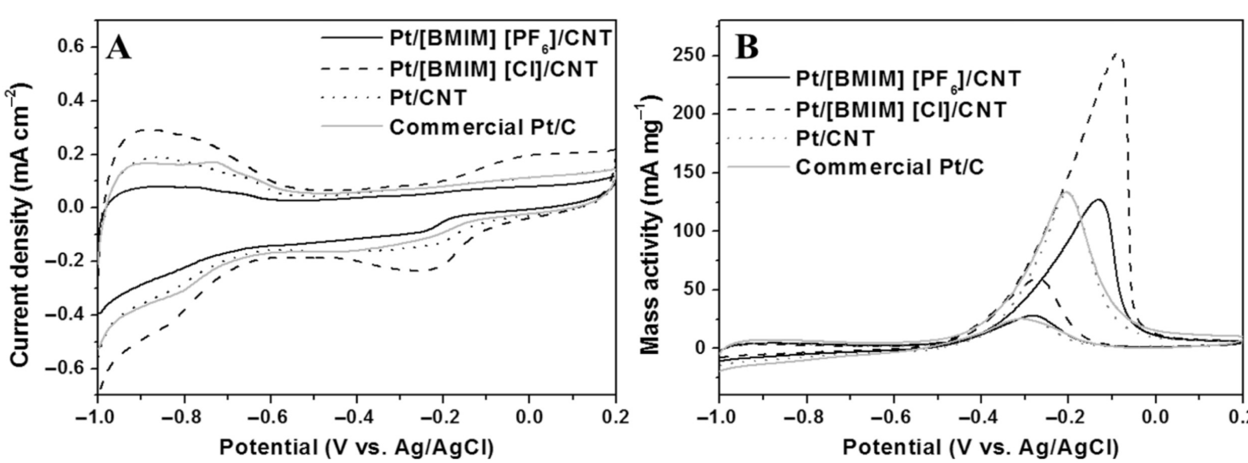

Figure 3. (A) EASA and (B) CV curves of Pt/[BMIM][PF_6]/CNT, Pt/[BMIM][Cl]/CNT, Pt/CNT nanohybrids, and commercial Pt/C NPs electrodes. (A) EASA was estimated by integrating the charges associated with hydrogen desorption in 0.5 M KOH. (B) CV was conducted in 0.5 M KOH containing 0.5 M methanol. Scan rate: 100 mV s^{-1}.

the Pt/[BMIM][Cl]/CNT nanohybrids resulted in the high electrocatalytic activity. Small sizes (large surface areas) of Pt NPs in the Pt/[BMIM][Cl]/CNT nanohybrids contributed to the improvement of their electrocatalytic activity toward MOR [47]. The voltammograms of Pt/CNT nanohybrids and commercial Pt/C are very similar, providing mass activities for MOR of 132.5 and 133.5 A g^{-1}, respectively. The higher mass activity and a lower onset potential obtained in the Pt/[BMIM][Cl]/CNT nanohybrid-electrode reveal that the Pt/[BMIM][Cl]/CNT nanohybrids provided greater electrooxidation activity toward MOR. During the MOR process, the adsorption of intermediate carbonaceous species on the catalyst's surface would lead to "catalyst poisoning." The ratio of the forward oxidation current peak (I_f) to the reverse current peak (I_b), I_f/I_b, is an important index of the catalyst tolerance to the carbonaceous species accumulation. A higher I_f/I_b ratio indicates that methanol is efficiently oxidized to CO_2 and a little accumulation of carbonaceous residues at the catalyst surface [48–51]. The I_f/I_b values of as-prepared catalysts were calculated to be 3.5 for Pt/[BMIM][PF_6]/CNT, 4.5 for Pt/[BMIM][Cl]/CNT, 2.8 for Pt/CNT, and 3.1 for commercial Pt/C. A higher I_f/I_b value of Pt/[BMIM][Cl]/CNT catalyst when compared with other reported catalysts (0.83 for Pt/CCG [27], 0.72 for Pt/MWCNT [27], and 1.75 for $Pt_{0.17}Cu_{0.83}$/graphene [29]) reveal that oxidation of methanol occurs more effectively. The enhanced electrocatalytic activity and stability for MOR of Pt/[BMIM][Cl]/CNT nanohybrids are probably due to the strong interactions between the [BMIM][Cl] and Pt NPs, which inhibit the formation of chemisorbed carbonaceous species [52]. To test the important role-playing by the counterions in determining the electroactivity, Pt/ILs/CNT nanohybrids prepared using [BMIM][Br] and [BMIM][I] were separately investigated (Figure S2A and S2B). The MOR current densities (8.5 and 9.9 mA cm^{-2}) provided by the two electrodes were lower than that of the Pt/[BMIM][Cl]/CNT electrode. Having higher viscosity than [BMIM][Cl], [BMIM][Br] and [BMIM][I] were difficultly dispersed on the CNT surface, leading to greater aggregation of Pt NPs. As a result, poor reproducibility was obtained.

The CVs displayed in Figure S3A and 3B reveal that the EASA values do not depend on the amounts of [BMIM][PF_6] but on the amount of [BMIM][Cl]. [BMIM][Cl] possessing hydrophilic property can adsorb H atoms more strongly than [BMIM][PF_6] does [53]. In other words, direct MOR processes would occur favorably on the as-prepared Pt/[BMIM][Cl]/CNT nanohybrid-modified electrodes, leading to greater catalytic activity. As expected, Figure S4A and 4B show that the amount of [BMIM][PF_6] in the Pt/[BMIM][PF_6]/CNT nanohybrids and that of [BMIM][Cl] in the Pt/[BMIM][Cl]/CNT nanohybrids does not and does affect their mass activities, respectively. Upon increasing the amount of [BMIM][Cl], greater amounts of Pt NPs were formed, leading to greater EASA values and thus mass activity. The optimum loading volume of [BMIM][Cl] was found to be 400 μL. Further increases in the amount of [BMIM][Cl] is not suggested, mainly because greater amounts of Pt NPs were not formed [11].

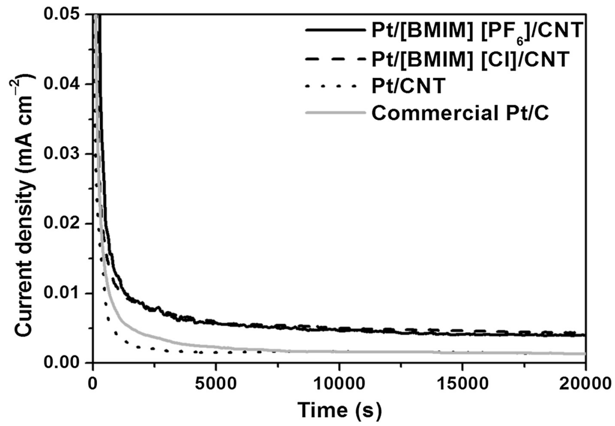

Figure 4. Chronoamperometric curves of Pt/[BMIM][PF_6]/CNT, Pt/[BMIM][Cl]/CNT, Pt/CNT nanohybrids, and commercial Pt/C NPs electrodes at a fixed potential of −0.1 V vs. Ag/AgCl in 0.5 M KOH containing 0.5 M methanol.

Further evaluation of the catalytic durability of as-prepared Pt/[BMIM][PF_6]/CNT, Pt/[BMIM][Cl]/CNT, Pt/CNT nanohybrids, and commercial Pt/C NPs electrodes was performed by chronoamperometry in 0.5 M KOH containing 0.5 M methanol at −0.1 V vs. Ag/AgCl. As shown in Figure 4, an initial decay of the current density occurred, mainly because of loss of surface active sites as a result of adsorption of intermediate species on the catalyst surface [54]. The as-synthesized Pt/[BMIM][Cl]/CNT and Pt/[BMIM][PF_6]/CNT catalysts provided greater stability (at least sweeping for 20,000 seconds) and higher current densities than the rest. These results reveal that the coordination of Pt with BMIM on the surfaces of CNTs did play a significant role in stabilizing the Pt NPs.

CONCLUSIONS

We have demonstrated a facile IL-assisted method for one-pot preparation of Pt/IL/CNTs nanohybrids, with high mass activity and long durability. Among four tested ILs, [BMIM][Cl] allowed preparation of the Pt/IL/CNTs that provided the highest mass activity. Our result reveals that the counterions play a significant role in determining the amounts of Pt NPs on the CNT support. In the presence of ILs, small sizes of Pt NPs on the CNT support were formed, leading to greater mass activity than other reported electrodes. Having advantages of good stability, excellent electrocatalytic activities, and cost effectiveness, the Pt/[BMIM][Cl]/CNT nanohybrids-modified electrode demonstrates great potential as an efficient anode catalyst for DMFCs.

SUPPLEMENTARY INFORMATION

Supplementary material is freely available **here**.

ACKNOWLEDGMENT

This study was financially supported by the Ministry of Science and Technology of Taiwan under contracts NSC 100-2627-M-002-007 and 101-2113-M-002-002-MY3. A. P. Periasamy is grateful to the Department of Chemistry, National Taiwan University for a postdoctoral fellowship under the contract number 101-R-4000.

REFERENCES

[1] Guo S, Dong S, Wang E. Constructing carbon nanotube/Pt nanoparticle hybrids using an imidazolium-salt-based ionic liquid as a linker. Adv Mater. 2010;22:1269–72. doi:10.1002/adma.200903379

[2] Wu B, Kuang Y, Zhang Y, Zhang X, Chen J. Carbonization of ionic liquid polymer-functionalized carbon nanotubes for high dispersion of PtRu nanoparticles and their electrocatalytic oxidation of methanol. J Mater Chem. 2012;22:13085–90. doi:10.1039/c2jm30547j

[3] Baughman RH, Zakhidov AA, de Heer WA. Carbon nanotubes – the route toward applications. Science. 2002;297:787–92. doi:10.1126/science.1060928

[4] Qu L, Dai L. Substrate-enhanced electroless deposition of metal nanoparticles on carbon nanotubes. J Am Chem Soc. 2005;127:10806–7. doi:10.1021/ja053479+

[5] Mackiewicz N, Surendran G, Remita H, Keita B, Zhang G, Nadjo L, Hage`Ge A, Doris E, Mioskowski C. Supramolecular self-assembly of amphiphiles on carbon nanotubes: a versatile strategy for the construction of CNT/metal nanohybrids, application to electrocatalysis. J Am Chem Soc 2008;130(26):8110–1. doi:10.1021/ja8026373

[6] Wu B, Hu D, Kuang Y, Liu B, Zhang X, Chen J. Functionalization of carbon nanotubes by an ionic-liquid polymer: dispersion of Pt and PtRu nanoparticles on carbon nanotubes and their electrocatalytic oxidation of methanol. Angew Chem Int Ed. 2009;48:4751–4. doi:10.1002/anie.200900899

[7] Kim Y-T, Ohshima K, Higashimine K, Uruga T, Takata M, Suematsu H, Mitani T. Fine size control of platinum on carbon nanotubes: from single atoms to clusters. Angew Chem Int Ed. 2006;118(3):421–425. doi:10.1002/ange.200501792

[8] Zhao Y, Yang X, Zhan L, Ou S, Tian J. High electrocatalytic activity of PtRu nanoparticles supported on starch-functionalized multi-walled carbon nanotubes for ethanol oxidation. J Mater Chem. 2011;21:4257–63. doi:10.1039/c0jm03892j

[9] Wildgoose GG, Banks CE, Compton RG. Metal nanoparticles and related materials supported on carbon nanotubes: methods and applications. Small. 2006;2:182–93. doi:10.1002/smll.200500324

[10] Xing Y. Synthesis and electrochemical characterization of uniformly-dispersed high loading Pt nanoparticles on sonochemically-treated carbon nanotubes. J Phys Chem B. 2004;108:19255–9. doi:10.1021/jp046697i

[11] Chu H, Shen Y, Lin L, Qin X, Feng G, Lin Z, Wang J, Liu H, Li Y. Ionic-liquid-assisted preparation of carbon nanotube-supported uniform noble metal nanoparticles and their enhanced catalytic performance. Adv Funct Mater. 2010;20(21):3747–52. doi:10.1002/adfm.201001240

[12] He Z, Chen J, Liu D, Zhou H, Kuang Y. Electrodeposition of Pt–Ru nanoparticles on carbon nanotubes and their electrocatalytic properties for methanol electrooxidation. Diamond Relat Mater. 2004;13:1764–70. doi:10.1016/j.diamond.2004.03.004

[13] Zhao Y, Fan L, Zhong H, Li Y, Yang S. Platinum nanoparticle clusters immobilized on multiwalled carbon nanotubes: electrodeposition and enhanced electrocatalytic activity for methanol oxidation. Adv Funct Mater. 2007;17:1537–1541. doi:10.1002/adfm.200600416

[14] Guo D-J, Li H-L. High dispersion and electrocatalytic properties of Pt nanoparticles on SWNT bundles. J Electroanal Chem. 2004;573:197–202.

[15] Liu P. Modifications of carbon nanotubes with polymers. Eur Polym J. 2005;41:2693–703. doi:10.1016/j.eurpolymj.2005.05.017

[16] Sayes CM, Liang F, Hudson JL, Mendez J, Guo W, Beach JM, Moore VC, Doyle CD, West JL, Billups WE, Ausman KD, Colvin VL. Functionalization density dependence of single-walled carbon nanotubes cytotoxicity in vitro. Toxicol Lett. 2006;161(2):135–42. doi:10.1016/j.toxlet.2005.08.011

[17] Meng L, Fu C, Lu Q. Advanced technology for functionalization of carbon nanotubes. Prog Nat Sci. 2009;19:801–10. doi:10.1016/j.pnsc.2008.08.011

[18] Suarez PAZ, Selbach VM, Dullius JEL, Einloft S, Piatnicki CMS, Azambuja DS, De Souza RF, Dupont J. Enlarged electrochemical window in dialkyl-imidazolium cation based room-temperature air and water-stable molten salts. Electrochim Acta. 1997;42(16):2533–5. doi:10.1016/S0013-4686(96)00444-6

[19] Zhang J, Bond AM. Conditions required to achieve the apparent equivalence of adhered solid- and solution-phase voltammetry for ferrocene and other redox-active solids in ionic liquids. Anal Chem. 2003;75:2694–702. doi:10.1021/ac026329f

[20] Wang Z, Zhang Q, Kuehner D, Xu X, Ivaska A, Niu L. The synthesis of ionic-liquid-functionalized multiwalled carbon nanotubes decorated with highly dispersed Au nanoparticles and their use in oxygen reduction by electrocatalysis. Carbon. 2008;46:1687–92. doi:10.1016/j.carbon.2008.07.020

[21] Tatumi R, Fujihara H. Remarkably stable gold nanoparticles functionalized with a zwitterionic liquid based on imidazolium sulfonate in a high concentration of aqueous electrolyte and ionic liquid. Chem Commun. 2005;1:83–5. doi:10.1039/b413385d

[22] Verwey EJW, Overbeek JTG. Theory of the stability of lyophobic colloids. New York: Dover Publications; 1999.

[23] Rodríguez-Cabo B, Rodil E, Soto A, Arce A. Preparation of metal oxide nanoparticles in ionic liquid medium. J Nanopart Res. 2012;14:1–10. doi:10.1007/s11051-012-0939-9

[24] Li Z, Jia Z, Luan Y, Mu T. Ionic liquids for synthesis of inorganic nanomaterials. Curr Opin Solid State Mater Sci. 2008;12:1–8. doi:10.1016/j.cossms.2009.01.002

[25] Zou H, Luan Y, Wang X, Xie Z, Liu J, Sun J, Wang Y, Li Z. Ionic liquid-assisted synthesis of carbon nanotube/platinum nanocomposites. J Nanopart Res. 2012;14(4):1–10. doi:10.1007/s11051-012-0832-6

[26] Sharma S, Ganguly A, Papakonstantinou P, Miao X, Li M, Hutchison JL, Delichatsios M, Ukleja S. Rapid microwave synthesis of CO tolerant reduced graphene oxide-supported platinum electrocatalysts for oxidation of methanol. J Phys Chem C. 2010;114(45):19459–66. doi:10.1021/jp107872z

[27] Li Y, Gao W, Ci L, Wang C, Ajayan PM. Catalytic performance of Pt nanoparticles on reduced graphene oxide for methanol electro-oxidation. Carbon. 2010;48:1124–30. doi:10.1016/j.carbon.2009.11.034

[28] Yang J, Deivaraj TC, Too H-P, Lee JY. Acetate stabilization of metal nanoparticles and its role in the preparation of metal nanoparticles in ethylene glycol. Langmuir. 2004;20:4241–5. doi:10.1021/la035088j

[29] Liu Y, Huang Y, Xie Y, Yang Z, Huang H, Zhou Q. Preparation of highly dispersed CuPt nanoparticles on ionic-liquid-assisted graphene sheets for direct methanol fuel cell. Chem Eng J. 2012;197:80–7. doi:10.1016/j.cej.2012.05.011

[30] Halder A, Sharma S, Hegde MS, Ravishankar N. Controlled attachment of ultrafine platinum nanoparticles on functionalized carbon nanotubes with high electrocatalytic activity for methanol oxidation. J Phys Chem C. 2009;113:1466–73. doi:10.1021/jp8072574

[31] Zhang H, Cui H. Synthesis and characterization of functionalized ionic liquid-stabilized metal (gold and platinum) nanoparticles and metal nanoparticle/carbon nanotube hybrids. Langmuir. 2009;25:2604–12. doi:10.1021/la803347h

[32] Ago H, Kugler T, Cacialli F, Salaneck WR, Shaffer MSP, Windle AH, Friend RH. Work functions and surface functional groups of multiwall carbon nanotubes. J Phys Chem B. 1999;103 (38):8116–21. doi:10.1021/jp991659y

[33] Díaz J, Paolicelli G, Ferrer S, Comin F. Separation of the sp^3 and sp^2 components in the C1s photoemission spectra of amorphous carbon films. Phys Rev B. 1996;54:8064–9. doi:10.1103/PhysRevB.54.8064

[34] Wang X, Fulvio PF, Baker GA, Veith GM, Unocic RR, Mahurin SM, Chi M, Dai S. Direct exfoliation of natural graphite into micrometre size few layers graphene sheets using ionic liquids. Chem Commun. 2010;46(25):4487–9. doi:10.1039/c0cc00799d

[35] Xu F, Minniti M, Barone P, Sindona A, Bonanno A, Oliva A. Nitrogen doping of single walled carbon nanotubes by low energy ion implantation. Carbon. 2008;46:1489–96. doi:10.1016/j.carbon.2008.06.047

[36] Yu P, Lin Y, Xiang L, Su L, Zhang J, Mao L. Molecular films of water-miscible ionic liquids formed on glassy carbon electrodes: characterization and electrochemical applications. Langmuir. 2005;21:9000–6. doi:10.1021/la051089v

[37] Liu N, Luo F, Wu H, Liu Y, Zhang C, Chen J. One-step ionic-liquid-assisted electrochemical synthesis of ionic-liquid-functionalized graphene sheets directly from graphite. Adv Funct Mater. 2008;18:1518–25. doi:10.1002/adfm.200700797

[38] Lin Z-H, Shih Z-Y, Tsai H-Y, Chang H-T. Gold/platinum nanosponges for electrocatalytic oxidation of methanol. Green Chem. 2011;13:1029–35. doi:10.1039/c0gc00648c

[39] Tan Y, Xu C, Chen G, Zheng N, Xie Q. A graphene–platinum nanoparticles–ionic liquid composite catalyst for methanol-tolerant oxygen reduction reaction. Energy Environ Sci. 2012;5:6923–7. doi:10.1039/c2ee21411c

[40] Liu Y, Huang Y, Xie Y, Yang Z, Huang H, Zhou Q. Preparation of highly dispersed CuPt nanoparticles on ionic-liquid-assisted graphene sheets for direct methanol fuel cell. Chem Eng J. 2012;197:80–7. doi:10.1016/j.cej.2012.05.011

[41] Wu B, Hu D, Kuang Y, Liu B, Zhang X, Chen J. Functionalization of carbon nanotubes by an ionic-liquid polymer: dispersion of Pt and PtRu nanoparticles on carbon nanotubes and their electrocatalytic oxidation of methanol. Angew Chem Int Ed. 2009;48: 4751–4. doi:10.1002/anie.200900899

[42] Yu H-E, Scott K, Reeve R-W. A study of the anodic oxidation of methanol on Pt in alkaline solutions. J Electroanal Chem. 2003;547:17–24. doi:10.1016/S0022-0728(03)00172-4

[43] Zhang J, Huang M, Ma H, Tian F, Pan W, Chen S. High catalytic activity of nanostructured Pd thin films electrochemically deposited on polycrystalline Pt and Au substrates towards electro-oxidation of methanol. Electrochem Commun 2007;9:1298–304. doi:10.1016/j.elecom.2007.01.038

[44] Markovic N, Ross P-N. The effect of specific adsorption of ions and underpotential deposition of copper on the electro-oxidation of methanol on platinum single-crystal surfaces. J Electroanal Chem. 1992;330:499–520. doi:10.1016/0022-0728 (92)80327-Z

[45] Yang L, Hu C, Wang J, Yang Z, Guo Y, Bai Z, et al. Facile synthesis of hollow palladium/copper alloyed nanocubes for formic acid oxidation. Chem Commun. 2011;47(30):8581–3. doi:10.1039/c1cc12528a

[46] Cochell T, Manthiram A. $Pt@Pd_xCu_y/C$ core–shell electrocatalysts for oxygen reduction reaction in fuel cells. Langmuir. 2011;28:1579–87. doi:10.1021/la202610z

[47] Hsin YL, Hwang KC, Yeh C-T. Poly(vinylpyrrolidone)-modified graphite carbon nanofibers as promising supports for PtRu catalysts in direct methanol fuel cells. J Am Chem Soc. 2007;129:9999–10010. doi:10.1021/ja072367a

[48] Zhao M, Li J, Song Z, Desmond R, Tschaen DM, Grabowski EJJ, Reider PJ. A novel chromium trioxide catalyzed oxidation of primary alcohols to the carboxylic acids. Tetrahedron Lett. 1998;39(30):5323–6. doi:10.1016/S0040-4039(98)00987-3

[49] Keresszegi C, Ferri D, Mallat T, Baiker A. Unraveling the surface reactions during liquid-phase oxidation of benzyl alcohol on Pd/Al_2O_3: an in Situ ATR−IR study. J Phys Chem B. 2004;109:958–67. doi:10.1021/jp0459864

[50] Abad A, Concepción P, Corma A, García H. A collaborative effect between gold and a support induces the selective oxidation of alcohols. Angew Chem Int Ed. 2005;44:4066–9. doi:10.1002/anie.200500382

[51] Choudhary VR, Dumbre DK, Bhargava SK. Oxidation of benzyl alcohol to benzaldehyde by tert-butyl hydroperoxide over nanogold supported on TiO_2 and other transition and rare-earth metal oxides. Ind Eng Chem Res. 2009;48:9471–8. doi:10.1021/ie801883d

[52] Li J, Lin X. A composite of polypyrrole nanowire: platinum modified electrode for oxygen reduction and methanol oxidation reactions. J Electrochem Soc. 2007;154:B1074–B9. doi:10.1149/1.2769820

[53] Anderson JL, Armstrong DW, Wei G-T. Ionic liquids in analytical chemistry. Anal Chem. 2006;78:2892–902. doi:10.1021/ac069394o

[54] Xu C, Liu Y, Wang J, Geng H, Qiu H. Nanoporous PdCu alloy for formic acid electro-oxidation. J Power Sources. 2012;199:124–31. doi:10.1016/j.jpowsour.2011.10.075

COMPETING FINANCIAL INTERESTS

The authors declare no competing financial interest.

PUBLISHING NOTES